

SEMI-EMPIRICAL INVESTIGATION OF ELECTRONIC, VIBRATIONAL AND THERMODYNAMIC PROPERTIES OF PERYLENE MOLECULE (C₂₀H₁₂)[†]

Abdul Hakim Sh. Mohammed^a, Issa Z Hassan^a, Hassan A. Kadhem^b,
Rosure Borhanalden Abdulrahman^{c*}

^aDepartment of Physics, college of Education for pure sciences, University of Kirkuk, Kirkuk, Iraq

^bMinistry of Education, Open Educational College, Kirkuk Center, Iraq

^cDepartment of Physics, College of Science, University of Kirkuk, Kirkuk, Iraq

*Corresponding Author: rabdulrahman@uokirkuk.edu.iq

Received December 20, 2022; revised January 29, 2023; accepted January 30, 2023

This work investigates computationally the spectroscopic and thermodynamics properties of the perylene molecule (C₂₀H₁₂) in the gas phase by utilizing a semi-empirical method [Hyper Chem8.0 and WinMopac7.0] programs, via (MNDO-PM3). This method is providing more simplicity and quick performance. The electronic properties such as total energy, dissociation energy, molecular orbital, ionization potentials, electronic affinity, and energy gap were calculated. However, vibration analysis and UV-visible spectra have been calculated. Moreover, the thermodynamic properties at the standard temperature such as heat of formation, entropy, enthalpy, heat capacity, and Gibbs free energy were calculated.

Keywords: Perylene; C₂₀H₁₂; Energy of molecule; UV-visible; IR; MNDO-PM3; Thermodynamic

PACS: 33.15.Ry, 33.15.-e, 31.10.+z, 65.40.gd, 65.40.Ba, 05.70.Ce, 05.70.Ce, 33.15.Dj, 33.20.Kf

INTRODUCTION

In the last few years, there has been an important effort in the preparation of new organic semiconductors for their application in electronics and optoelectronic devices. Specifically, the development of novel organic semiconductors with effective charge transport capability is an attractive topic in the field of organic electronics for many applications such as organic thin-film transistors (OTFT) and organic light-emitting diodes (OLED) [1–4]. Current and future applications of organic semiconductors range from commercially available OLED displays [5], and infrared applications [6–7], over potentially printable organic [8] and hybrid organic/inorganic solar cells [9], to printable electronic circuits based on organic field-effect transistors (OFET) [10]. While OLED displays outperform their inorganic counterparts in terms of energy efficiency [11]. Compared to inorganic materials, the use of organic semiconductors are attractive because these materials offer many advantages, for example, low cost and the ability to form thin films, which enable the fabrication of large-area and flexible devices. Organic semiconductors include both small molecules and polymers, small molecules have advantages such as easier synthetic procedures, purification methods, and characterization in view of their small size and well-defined structure [12]. In addition, their optical and electronic properties can be easily tuned by means of molecular design. Nature has conserved an infinite variety of organic chemicals, and these materials have much better ranges for ease of making, shaping, and adjusting the properties of materials compared to inorganic chemicals [13]. π - π stacking of organic chemicals reveals good conductivity of charge carriers [13–14]. Regarding the optical performance, the nano/sub-micron organic structures showed a quantum yield close to that of photoluminescence [15]. Subsequently, organic single crystals with excellent optical and electrical properties are critical for the development of organic optoelectronics [16].

Perylene is a brown solid that is a multi-cyclic aromatic hydrocarbon with the chemical formula C₂₀H₁₂. It exhibits blue fluorescence and is utilized as a pure or substituted blue-emitting dopant material in OLEDs. Perylene is also utilized as an organic photoconductor and has been used as technical dyes for many years attributed to its high temperature, photo, and chemical constancy [17]. Besides that, in the last years, such compounds gained large widespread because of their use in optical devices [18–19]. These π conjugated dyes show high photosensitivity and high electron mobility [20–21]. As well as photo physical properties, particularly the sensitivity of their fluorescence lifetime to the PH, render them very useful as probes for live-cell fluorescence lifetime imaging [22]. Perylene dyes are a representative framework of electron transport (n-type) organic semiconductors. The energy of their electron transport level is the electron affinity (EA), which is an important parameter in selecting the electron transport materials for device application and the material's electron-accepting ability [23].

The research employed semi-empirical programs that had fast computational cycles. One of these semi-empirical methods is the MNDO-PM3 approach, which calculates the experimentally measured practical values. This program has adopted one of the molecular modeling methods (HyperChem8.0), and by means of the molecules are drawn in a preliminary way, while fixing the nature of the bonds between two atoms of the molecule. Additionally, the spatial geometry of the molecule is calculated to the nearest energy –stable geometric shape by conducting the process of

[†] Cite as: A.H.Sh. Mohammed, I.Z. Hassan, H.A. Kadhem, and R.B. Abdulrahman, East Eur. J. Phys. 1, 210 (2023), <https://doi.org/10.26565/2312-4334-2023-1-28>

© A.H.S. Mohammed, I.Z. Hassan, H.A. Kadhem, R.B. Abdulrahman, 2023

reducing energy to the optimum limit (Geometry optimization). The potential energy curve is drawn by changing the length of the bond between the two atoms and keeping the total energy at each change as low as possible. Quasi-experimental methodologies are based on the electronic Schrödinger equation gained after detach the nuclear and electronic motion, (Born-Oppenheimer approximation)

$$\hat{H}(r, R) \Psi(r, R) = E(r, R) \Psi(r, R). \quad (1)$$

Here r and R indicate the coordinates of the electrons and the nucleus respectively [24].

This study's aim is to investigate Perylene's ($C_{20}H_{12}$) vibration spectrum and electronic structure in the IR region and electronic transition in the UV-visible region, using semi-empirical calculations (MNDO-PM3). It has a planar structure with D_{2h} point symmetry. The research purpose to calculate the lower energy of the stabilized state of the molecule way potential energy curves. One important characteristics that have been studied are for the thermodynamic principles which is concerned with the energy transformation of the substance in the empty space that the substance occupies (system) and the subsequent shift in its energy level the internal energy is a type of potential energy in the system which plays a role in many concepts, including heat capacity its unit $\text{cal.mol}^{-1}.\text{deg}^{-1}$ [25], All materials have an enthalpy that depends on pressure, temperature, and internal energy, with the exception of gases, which behave ideally or almost ideally [26]. The distinctive characteristic that relates to the stability of the compound is either the heat of formation or the enthalpy of formation; if it is positive, the compound is unstable, and if it is negative the compound is stable. Entropy (S), which it is a measure of the resulting randomness of a compound due to the change in temperature degrees, is another function [27]. Additionally, free Gibbs energies were calculated using the [HyperChem8.0 and WinMopac7.0] software.

COMPUTATION METHODS

Semi-empirical calculation investigations were carried out using MNDO-PM3 in order to understand the geometrical optimization and electron structures of perylene in the neutral and singlet states. Computation the electronic properties like the ionization energy of electronic states, and energy gap (E_g), geometric optimization of Perylene in the gas phase by the semi-empirical way, and calculated the highest occupied molecular orbital in electron (HOMO) and lowest unoccupied molecular orbital in electron (LUMO). In addition, computation of the IR spectrum in the ground state, ionization potential (IP) and electronic affinity (EA) by using the following equations [28],

$$IP = |E_{\text{HOMO}}| \quad ; \quad EA = |E_{\text{LUMO}}| \quad (2)$$

Also, the electronegativity (χ) has been computed by using the equation [29],

$$\chi = (IP + EA) / 2 \quad (3)$$

While the hardness (η) is defined [29],

$$\eta = (IP - EA) / 2 \quad (4)$$

Whereas the softness (S) and electrophilic (W) is defined by equations [30],

$$S = 1 / 2 \eta \quad (5)$$

$$W = \chi^2 / 2\eta \quad (6)$$

Several thermodynamic properties of the perylene molecule have been investigated using computer programs (WinMopac 7.0). These properties determine the most important conditions for conducting reactions as well as the effect of temperatures on a molecule within the three phases and for a variety of temperatures that include melting, boiling, and standard degrees, as well as comparing the results with experimental values taken from the literature.

RESULTS AND DISCUSSION

Molecular Structure

The geometric shape of the perylene molecule ($C_{20}H_{12}$) was drawn through a program HyperChem8.0 that relies on calculating the internal coordinate (r, θ, ϕ) and on the geometric form at the equilibrium case of the perylene as in Figure 1.

After getting the matrix and inserting it into the program WinMopac 7.0, some important properties of the perylene molecule were determined, such as the final heat of formation, the total energy at the stability posture, the binding energy, the electronic energy, the core-core interaction, the zero-point energy, the ionization potential, and the electronic affinity, as shown in Table 1.

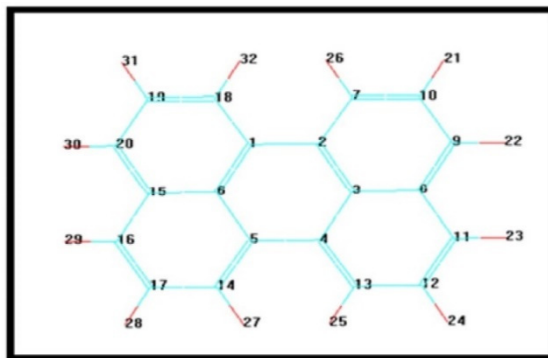


Figure 1. shows the molecular structure of the perylene molecule that was drawn in the program HyperChe8.0.

Table 1. show the result of some important properties of the perylene molecule was calculated, by using (HyperChem8.0 and WinMopac7.0)

Quantum	Magnitude Cal. [HyperChem8.0]	Magnitude Cal. [WinMopac 7.0]	Unit
Total Energy	-58880.6822330	-58879.1031898	/mol kcal
Total Energy	- 93.832328265		a.u.
Binding Energy	- 3961.4641970		kcal/mol
Isolated atomic energy	- 54919.2180360		kcal/mol
Electronic Energy	- 429071.4512403	-429045.60781474	kcal / mol
Core-Core Interaction	370190.7690073	370166.5046249	kcal / mol
Heat of Formation	81.5598030	82.019799	kcal/mol
Gradient	0.1844568	1.65705	mol/angkcal/
Molecular point group	D _{2h}		
Zero point energy of vibration	160.43560	160.886	kcal/mol
Ionization Potential	7.984057	7.98706	eV
Electronic Affinity	7.984		eV

The Un-Harmonic Potential Energy Calculation (Perylene)

Studying the potential curve, which represents the correlation between the total energy of the molecule and the interatomic distance of the active bonds in the perylene molecule, permitted to determine the lowest energy value of the curve, which represents the equilibrium point (the bottom of the curve). At the distance of ($r_e=1.1\text{Å}$), it has a value of (-3961.55) kcal/mol for (C10-H21) and (-3962.5510) kcal/mol for (C17-H28).

The potential curve depicted the force between the atoms (C10-H21) and (C17-H28) for perylene, and these forces illustrate the total of the forces of repulsion and attraction. When the distance between the atoms is reduced, the force of attraction from the other nucleus begins to effect each electron. At the same time, electrons and nuclei begin to repel each other [31]. When the atoms are separated from each other by increasing the distance, the gravitational force will present that the total energy decreases due to the decrease in the potential energy and the electronic-nucleus attraction, thus; increasing the energy reduction until it reaches the lowest total energy value. The dissociation energy of the molecule is calculated from the difference between its lowest energy value and its value when r is infinity. Furthermore, when the distance between two atoms is infinite, the potential energy becomes zero [31], and the value of dissociation energy is as follows: (C10-H21) ($D_e = 182.44$ kcal/mol.) as shown in Figure 2, and (C17-H28) ($D_e = 209.08$ kcal/mol.) illustrated in Figure 3.

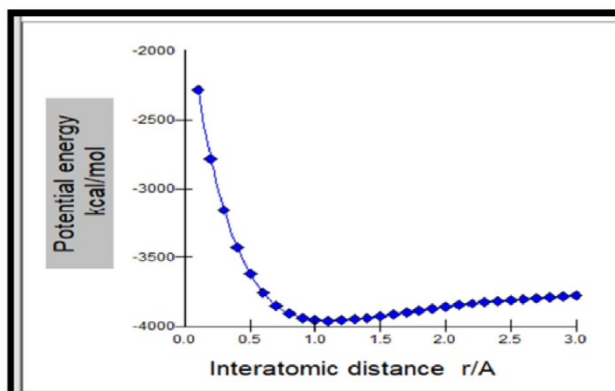


Figure 2. Potential energy change with interatomic distance (C10-H21) of perylene molecule.

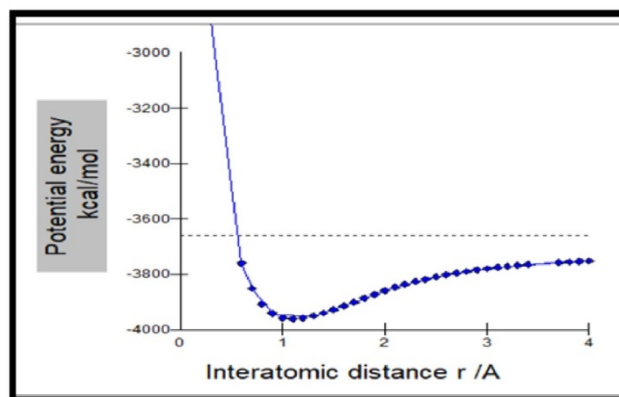


Figure 3. potential energy change with interatomic distance (C17-H28) of perylene molecule.

Calculation the Vibrational Frequencies of the Perylene Molecule

After drawing the potential energy curve of the molecule at the equilibrium position, the modes of vibration frequencies of the molecule were calculated from this point, which was 90 modes according to $(3N-9)$ and by using (HyperChem 8.0 and WinMopac 7.0) expressed in wavenumber and unit cm^{-1} . The results showed that the calculated values were close to practical and theoretical values in the literature, as shown in Table 2.

Table 2. vibrational frequencies of perylene calculated by using (HyperChem8.0 and WinMopac7.0) programs and Comparison with practical values and other works.

Vibe. modes	Symmetry	Intensity	Wave number 1/cm Cal. [HyperChem]	Wavenumber 1/cm Cal. [WinMopac]	Cal. cm^{-1}	Exp. Cm^{-1}	Cal. cm^{-1}
					[32]	[33]	
1	1 AU	0.00006	49.04	49.425			
2	1 B3U	0.23811	90.03	91.21			87
3	1 B2G	0	150.68	151.32			126
4	2 B3U	2.54259	166.98	167.51			172
5	1 B1G	0	181.7	182.2			188
6	2 AU	0	230.8	231.36			255
7	2 B2G	0	286.72	287.01			
8	1 B2U	0.01594	287.56	287.76			294
9	1 B3G	0	368.67	368.71			368
10	1 AG	0	381.64	381.67			
11	2 B1G	0	385.77	386.22			403
12	3 B3U	0.09547	428.46	428.76			
13	3 B2G	0.00001	436.79	436.98			441
14	2 AG	0	462.17	462.47			445
15	3 AU	0.00001	480.37	480.56			482
16	1 B1U	0.13799	486.95	487.11			
17	4 B3U	4.4721	538.12	538.4			534
18	2 B2U	0.16382	545.65	545.67			546
19	3 B1G	0	559.21	559.48			
20	2 B3G	0	562.44	562.52			
21	2 B1U	0.39825	592.71	592.84			581
22	4 B2G	0	636.49	636.58			
23	3 AG	0	637.91	637.97			
24	3 B3G	0	651.22	651.26			642
25	4 AU	0.00022	673.88	674.12			685
26	4 B1G	0.0029	777.76	777.8			773
27	5 B3U	55.62972	778.42	778.54			
28	5 B2G	0	796.71	796.87	794	794	793
29	3 B2U	0.11724	797.61	797.72			
30	5 AU	0.00011	798.94	799.08			
31	3 B1U	0.87439	810.99	811.08			815
32	4 AG	0	823.37	823.46			
33	6 B3U	28.1843	849	849.08			853
34	6 B2G	0	894.95	895.13			
35	5 B1G	0	912.18	912.34			910

Vibe. modes	Symmetry	Intensity	Wave number 1/cm Cal. [HyperChem]	Wavenumber 1/cm Cal. [WinMopac]	Cal. cm ⁻¹	Exp. Cm ⁻¹	Cal. cm ⁻¹
					[32]		[33]
36	7 B3U	0.00045	931.92	932.1			
37	6 AU	0.00011	938.39	938.52			938
38	4 B3G	0	940.27	940.37			940
39	7 B2G	0	960.19	960.36			968
40	4 B1U	0.15287	979.57	979.74			969
41	6 B1G	0	990.69	990.83			983
42	7 AU	0.00011	1001.73	1001.89			
43	8 B3U	3.99791	1006.18	1006.28			
44	8 B2G	0	1015.28	1015.39	1018		1020
45	5 AG	0	1082.89	1083.24			1091
46	5 B3G	0	1117.67	1117.72	1110	1112	
47	4 B2U	0.045	1129.57	1129.97			
48	5 B1U	0.45894	1134.18	1134.36			
49	5 B2U	0.44051	1134.57	1134.66			
50	6 B3G	0	1146.16	1146.71			
51	6 B1U	0.02615	1148.13	1148.54			
52	6 AG	0	1163.26	1163.35	1182	1191	1177
53	7 B3G	0	1196.58	1196.73			1184
54	6 B2U	0.92369	1209.41	1209.6			
55	7 B1U	0.06871	1213.37	1213.6	1204	1217	1218
56	7 AG	0	1261.18	1261.34			1241
57	8 B3G	2.01679	1265.9	1265.74	1279	1284	1264
58	7 B2U	0.02091	1318.88	1318.24	1320	1313	1315
59	8 B2U	0.00078	1324.37	1324.55			
60	8 AG	0	1346.39	1346.56	1369	1374	1355
61	8 B1U	13.78876	1430.71	1430.95			
62	9 B3G	0	1442.99	1442.72			1435
63	9 AG	0	1460.48	1460.73			
64	9 B2U	8.0757	1469.06	1469.07			1471
65	9 B1U	4.89914	1499.86	1500.13			1521
66	10 AG	0.00004	1569.98	1570.41	1542	1532	
67	10 B1U	0.74697	1575.75	1576.11			
68	10 B3G	0	1594.93	1595.11			1583
69	11 AG	0	1598.91	1599.06			1586
70	10 B2U	0.96029	1635.18	1635.35			1628
71	11 B3G	0	1694.65	1694.91			
72	11 B2U	0.09353	1720.86	1721.07			
73	11 B1U	0.51825	1784.28	1784.43			
74	12 AG	0.00012	1784.78	1784.93			
75	13 AG	0	1791.74	1791.87			
76	12 B1U	2.03035	1797.88	1798.02			
77	12 B2U	0.14084	1813.14	1813.29			
78	12 B3G	0	1827.36	1827.52			
79	25.09984	25.09984	3002.33	3002.33			
80	14 AG	0.00008	3002.23	3002.44			
81	13 B1U	1.26978	3018.79	3019.05			
82	13 B3G	0.00001	3018.9	3019.13			3031
83	15 AG	0.03805	3052.61	3053.16			3040
84	14 B1U	19.16395	3052.61	3053.17			3041
85	14 B3G	0.00305	3053.8	3054.35			
86	14 B2U	9.8558	3053.82	3054.37			3061
87	15 B1U	37.8511	3070.76	3071.35			3063
88	16 AG	0.00049	3070.95	3071.52			3065
89	15 B2U	29.08017	3071.15	3071.75			
90	15 B3G	0.00002	3071.22	3071.81			

We conclude from the above table that the vibration between the atoms (C-H) at the wavenumber (796.71 cm⁻¹) [32] is close to the results of the measured literature, both experimentally and theoretically, and is equal to 794 cm⁻¹, which is also consistent with previous studies (793 cm⁻¹) [33]. To describe the vibration modes of the perylene molecule HyperChem8.0 a program was used, as the molecule is drawn and the special main axes are determined for being a non-linear molecule. According to the rule (3N-6), we get 90 basic vibrational frequencies, and these modes were described

through the program by clarifying the directions of vibration of the atoms with arrows with an indication of the intensity, and the symmetry of each mode, as shown in Figure 4.

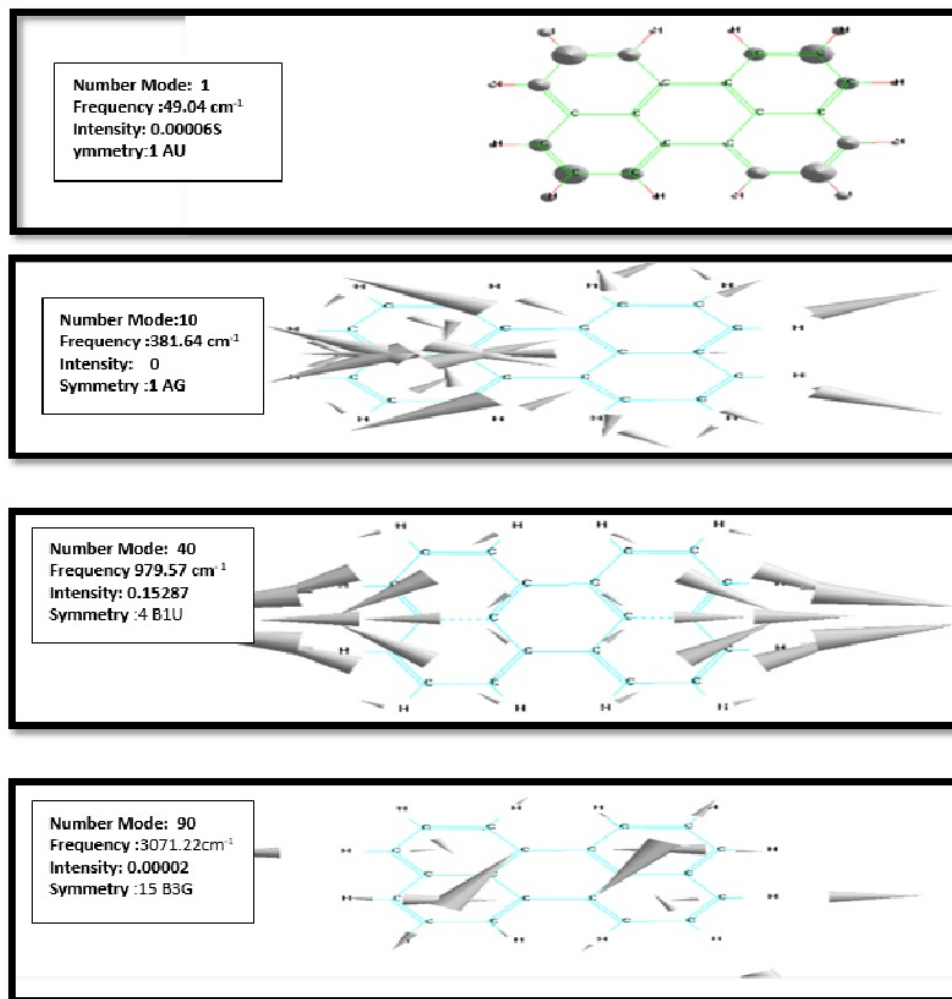


Figure 4. the basic vibrational modes of the perylene molecule were drawn using the HyperChem8.0 program, explaining the intensity, frequency and symmetry.

The Eigenvalues of the Orbitals of the Perylene Molecule

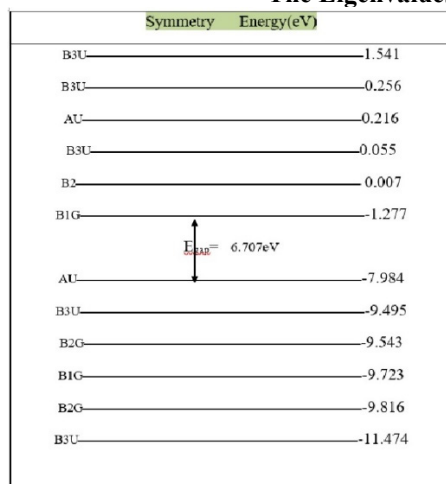


Figure 5. shows the values of the energy levels of the perylene molecule, showing the highest occupied molecular orbital (EHOMO) and the lowest unoccupied orbital (ELUMO), and the symmetry of each orbital calculated through the program HyperChem8.0

The energy levels of the perylene molecule were plotted using HyperChem8.0 software after the stable shape of the molecule was obtained, and the energy values for the highest occupied molecular orbital were equal to EHO-MO = -1.277 eV and the lowest unoccupied molecular orbital, ELUMO = -7.984 eV, and the symmetry of each orbit is shown in Figure 5. 46 was the number of orbitals occupied by the electrons, and 46 orbitals were unoccupied by the electrons. through which the energy gap between the two levels can be calculated ($E_g = \text{ELUMO} - \text{EHOMO}$) and is equal to 6.707 eV.

Electronic Properties of Perylene

After calculated the values of HOMO and LUMO for perylene molecules (C₂₀H₁₂), also calculated electronic properties (EA, IP) and calculated the global chemical indices such as (S, W, χ , η) by used semi-empirical way (MNDO-PM3) and was (IP=7.984eV), (EA=1.277eV), (χ =4.6309eV), (η =3.3535eV), (S=1.6767eV) and (W=3.197eV). By using equations 2, 3, 4, and 5 respectively. Additional to previous study we can also calculate the parameter for total charge density and electrostatic potential, illustrated in (2D contours) as shown in Figure 6.

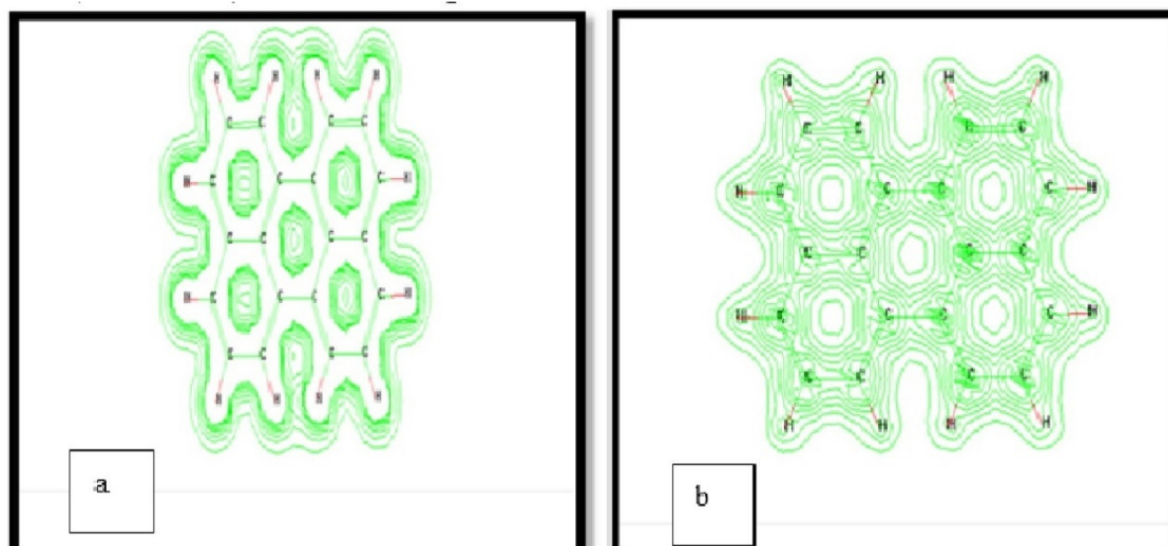


Figure 6. illustrated a- Electrostatic potential, b- Total charge density for perylene.

As we noticed from Figure 6b, the electronic charge density was centralized around the carbon atoms in the perylene molecule, in which the carbon atom is more negativity than the hydrogen atom. Figure 6a illustrates the electrostatic potential, which shows the plot of a contour map in 2D.

UV-Vis Spectroscopy of Perylene

The electronic transition was computed using the semi-empirical electronic spectrum from the configuration interaction (CI) method using the HyperChem8.0 program after obtaining the best balanced and stable geometric shape of the perylene molecule. Figure 7 depicts the absorption spectra, which exhibit two different bands (Q-band and B-band). The Q-band was found to be 412.3 nm, which is due to the π - π^* transition from the highest occupied molecular orbital (HOMO) to the lowest unoccupied molecular orbital (LUMO); this value agreed with previous studies, which found the Q-band to be 435 nm [34]. The B-band was identified to be 239.6 nm due to the transition from π levels to LUMO. Table 3 shows the absorbance range calculated between 180 and 650 nm.

Table 3. show the electron transition of perylene

Wavelength(nm)	Oscillator strength abs.
621.2	0
421.3	0.6192
346.8	0
343.9	0
334	0
332.4	0
323.8	0.0135
318.1	0
315.6	0
311.5	0
267.8	0
239.6	2.1082
235.5	1.5731
228.8	0
185.9	0
185.9	0
185.8	0.0006
185.8	0

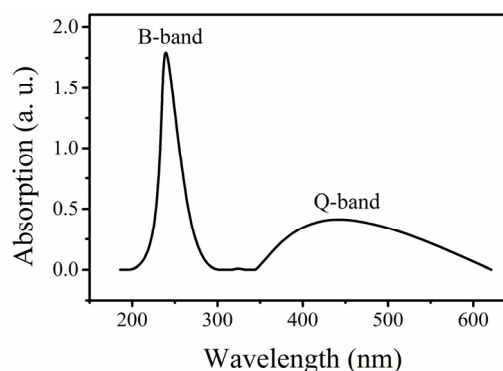


Figure 7. Absorption spectra of Perylene calculated by HyuperChem8.0 program

Thermodynamic Properties of Perylene Molecule

One of the important properties that have been studied is the thermal properties of the perylene molecule, which determine the most important conditions on the basis of which chemical reactions take place. After getting the energetically stationary shape of the molecule and obtaining the final matrix containing the charges of the atoms that make up the molecule through the WinMopac7.0 program, The MNDO-PM3 method has been used to obtain thermal functions during the three phases of the molecule, and for a number of temperatures that involve melting, boiling, and standard degrees, the dimensions between these atoms (r), the best position of these atoms (Opt.), the values of the angles (θ°) and the angles of the diagonal (α) are shown in Table 4.

Table 4. The final matrix of the perylene molecule is obtained from the WinMopac7.0, showing the interior coordinates (r , θ° , φ°) in the balance condition.

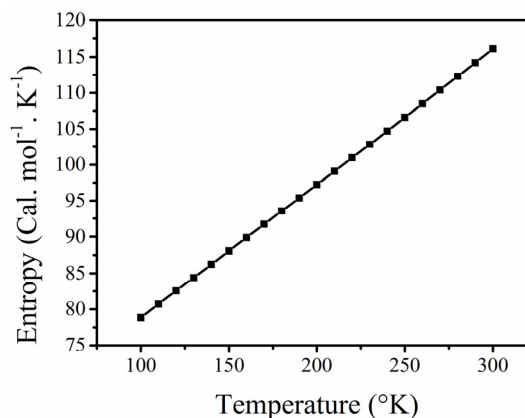
Atom	Distance	Opt.	Angle(θ°)	Opt.	Dihedral(φ°)	Opt.	A	B	C	Charge
C	.0000000	0	.000000	0	.000000	0	0	0	0	-.0148
C	1.4614239	1	.000000	0	.000000	0	0	0	0	-.0148
C	1.4269000	1	119.281700	1	.000000	0	2	1	0	-.0084
C	1.4268761	1	121.436500	1	.000000	1	3	2	1	-.0148
C	1.4614000	1	119.281700	1	.001296	1	4	3	2	-.0148
C	1.4269239	1	119.281700	1	.000000	1	1	2	3	-.0084
C	1.3796000	1	121.199400	1	179.999900	1	2	1	5	-.0997
C	1.4112239	1	119.281700	1	179.999900	1	3	2	1	-.0366
C	1.4201239	1	119.634900	1	.000000	1	8	3	2	-.0869
C	1.3692000	1	120.224400	1	-.001398	1	9	8	3	-.0970
C	1.4201000	1	119.633530	1	179.999900	1	8	3	2	-.0869
C	1.3692001	1	120.223029	1	.000000	1	11	8	3	-.0970
C	1.3796000	1	119.518777	1	.000000	1	4	3	8	-.0997
C	1.3796000	1	121.199400	1	.000000	1	5	4	3	-.0997
C	1.4112239	1	119.281700	1	179.999095	1	6	1	2	-.0366
C	1.4201239	1	119.634900	1	179.999900	1	15	6	1	-.0870
C	1.3692000	1	120.224500	1	-179.998899	1	16	15	6	-.0970
C	1.3796000	1	121.199400	1	.001170	1	1	2	7	-.0997
C	1.4091761	1	120.944600	1	.000000	1	18	1	6	-.0970
C	1.3692239	1	120.395300	1	.000000	1	19	18	1	-.0869
H	1.0949000	1	120.579301	1	179.999900	1	10	9	8	.1038
H	1.0957001	1	118.928407	1	179.999900	1	9	8	3	.1059
H	1.0957001	1	118.928408	1	179.999900	1	11	8	3	.1059
H	1.0949000	1	120.579197	1	179.999900	1	12	11	8	.1038
H	1.1011000	1	119.346230	1	179.999900	1	13	4	3	.1113
H	1.1011000	1	119.346330	1	179.999900	1	7	2	3	.1113
H	1.1011000	1	119.346230	1	179.999900	1	14	5	6	.1113
H	1.0949000	1	120.577930	1	179.999900	1	17	16	15	.1038
H	1.0957001	1	118.928403	1	179.999900	1	16	15	6	.1059
H	1.0957000	1	120.846999	1	179.999900	1	20	19	18	.1059
H	1.0949000	1	119.025200	1	179.999900	1	19	18	1	.1038
H	1.1011000	1	119.347700	1	179.999900	1	18	1	6	.1113

Heat of Formation

The heat of formation was computed for the perylene molecule in its energy-stable form and for various temperatures ranging from 100 to 300 °K (Table 5), as it included both the boiling and melting points as well as the standard temperature. Figure 8 shows that the heat of formation is temperature dependent and increases as temperature increases. The heat of formation at the standard temperature of 298 °K is 82 kcal.mol⁻¹, which is close to the result measured in the literature, which was 72.17 kcal.mol⁻¹ [35].

Table 5. The values of the heat of formation for the perylene molecule and their corresponding temperature

Temperature (K)	H. O. F. (kcal/mol)
100	74.641
110	74.839
120	75.052
130	75.282
140	75.53
150	75.794
160	76.077
170	76.379
180	76.7
190	77.04
200	77.4
210	77.781
220	78.181
230	78.603
240	79.044
250	79.507
260	79.991
270	80.495
280	81.021
290	81.568
300	82.135

**Figure 9.** The relationship between the entropy of the Perylene molecule and temperature

Entropy

Among the thermal properties that were calculated is the entropy for different temperatures to describe the randomness of the compound during the three phases, and the entropy value at the standard degree was 298K by (116) $\text{Cal}\cdot\text{mol}^{-1}\cdot\text{K}^{-1}$, which is close to the measured value from previous studies (112.14) $\text{Cal}\cdot\text{mol}^{-1}\cdot\text{K}^{-1}$ [35]. The randomness of the molecule begins to increase with increasing temperature as shown in Figure 9 and Table 6.

Table 6. the values of the entropy for the perylene molecule and their corresponding temperature

Temperature (K)	Entropy ($\text{Cal}\cdot\text{K}^{-1}\cdot\text{mol}^{-1}$)
100	78.8275
110	80.7091
120	82.5651
130	84.4049
140	86.2354
150	88.0617
160	89.8877
170	91.7162
180	93.5495
190	95.3889
200	97.2356
210	99.0904
220	100.9535
230	102.8253
240	104.7056
250	106.5943
260	108.4909
270	110.3951
280	112.3062
290	114.2237
300	116.1468

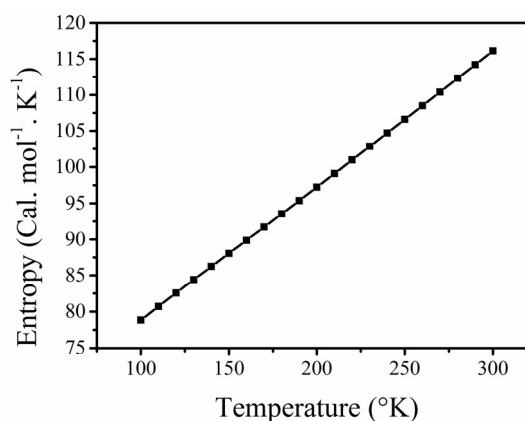


Figure 9. The relationship between the entropy of the Perylene molecule and temperature

Heat Capacity

The heat capacity of the perylene is a function of temperature and is directly proportional to it, as the increase in temperature increases the number of particles in the upper vibration energy level, and the heat capacity increases with constant pressure. At a temperature of 298 K and a pressure of 1 atmosphere, the heat capacity was 57.2 $\text{Cal}\cdot\text{mol}^{-1}\cdot\text{K}^{-1}$, which is close to the practical value of 49.13 $\text{Cal}\cdot\text{mol}^{-1}\cdot\text{K}^{-1}$ [35]. The heat capacity was also calculated for different values of temperature (100–300 °K) as shown in Figure 10 and Table 7.

Table 7. Shows the values between the heat capacity and temperature of perylene molecule

Temperature (K)	H. Capacity ($\text{Cal}\cdot\text{mol}^{-1}\cdot\text{K}^{-1}$)
100	18.9841
110	20.5394
120	22.1614
130	23.8464
140	25.5897
150	27.3865
160	29.2322
170	31.1223
180	33.0524
190	35.0182
200	37.0154
210	39.0396
220	41.0866
230	43.1519
240	45.2312
250	47.3203
260	49.415
270	51.5115
280	53.6057
290	55.6942
300	57.7737

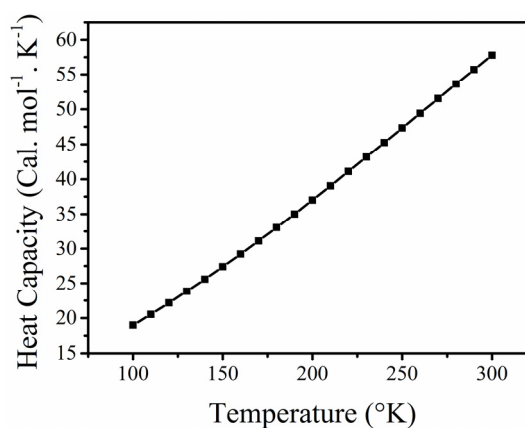


Figure 10. The relationship between heat capacity of perylene molecule and temperature

Enthalpy

The enthalpy function was determined for a variety of temperatures (Table 8) and represents the sum of the system's internal and external energy. and its value at standard temperature was $8740 \text{ Cal}\cdot\text{mol}^{-1}$, which is near to the sources determined by other methods, which were equal to $9080 \text{ Cal}\cdot\text{mol}^{-1}$, as shown in Figure 11. We observe that the enthalpy increases with rising temperature, demonstrating that the enthalpy is temperature dependent.

Table 8. Shows the values between the enthalpy and temperature of perylene molecule

Temperature (K)	Enthalpy (Cal.mol ⁻¹)
100	1248.9206
110	1446.4812
120	1659.9307
130	1889.919
140	2137.0529
150	2401.8915
160	2684.9465
170	2986.6841
180	3307.5262
190	3647.8512
200	4007.9947
210	4388.2489
220	4788.8627
230	5210.0414
240	5651.9468
250	6114.6978
260	6598.3715
270	7103.0042
280	7628.5934
290	8175.0994
300	8742.4478

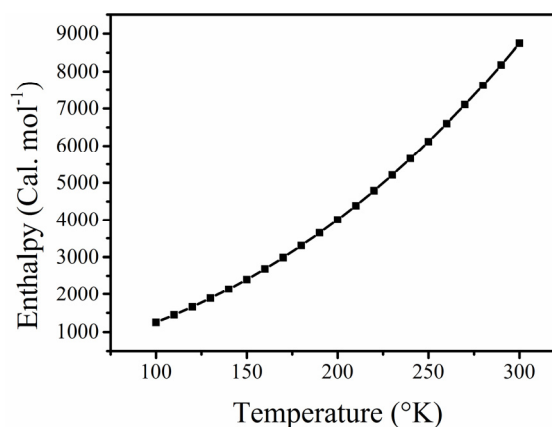


Figure 11. The relationship between the enthalpy and Perylene temperature

Gibbs Free Energy

After the change in entropy and enthalpy was calculated for the temperature range of 100–300 °K (Table 9) of the perylene molecule, the free energy of Gibbs was calculated in order to determine whether the reaction occurs spontaneously or not, using the equation ($\Delta G = \Delta E - T\Delta S$) and for the same temperatures. and it was at the standard temperature of $-2600.7 \text{ Cal}\cdot\text{mol}^{-1}$, and the relation between Gibbs's energy and temperature was drawn as in Figure 12. And the relationship was inverse between the two values; as the temperature increased, the free energy of Gibbs gradually decreased.

Table 9. the Gibbs free energy values of perylene molecule and the corresponding temperature

Temperature (K)	Gibbs=H-TS (Cal.mol)
100	-6633.8291
110	-7431.189
120	-8247.8813
130	-9082.718
140	-9935.90371
150	-10807.3635
160	-11697.0855
170	-12605.099
180	-13531.3838
190	-14476.3098
200	-15439.2053
210	-16420.7351
220	-17420.9073
230	-18439.7776
240	-19477.3972
250	-20533.8772
260	-21609.2625
270	-22703.6728
280	-23817.1426
290	-24949.7736
300	-26101.5922

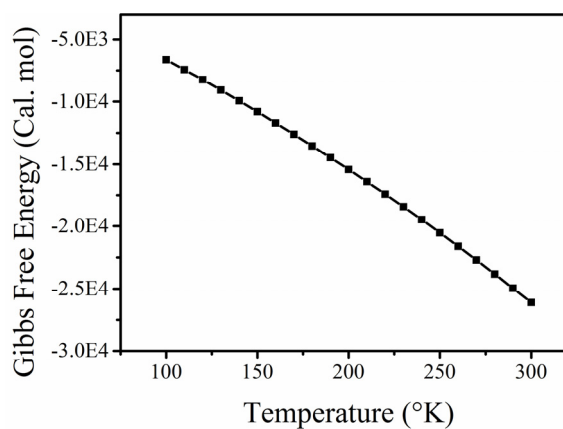


Figure 12. Show the relation between the Gibbs free energy and temperature of perylene molecule

CONCLUSIONS

The present study, show the results, that the (C-H) bond is the active bond in the molecule and the lowest energy of the perylene molecule to keep the molecule in a stable state was (-3961.45 eV). The equilibrium distance of the molecule was equal (1.1Å), and the dissociation energy of the molecule (C10-H21) was found to be (De = 182.44 kcal/mol.) and (C17-H28) (De = 209.08 kcal/mol. We conclude that the molecule begins to dissociate when the length of the bond breaks down and the energy at this point called the dissociation energy. With regard to the thermal properties, we note the direct proportionality of (ΔH_f , CP, H, S) with temperature and the interpretation of this according to quantum mechanics, as the thermal energies arising from both the transitional movement and the rotational and vibrational motion of the molecule are quantum energies and all of them are directly proportional to the temperature. As for high temperatures, electronic movement plays an important role, as high energies cause electronic transitions. Also, the increase in the values of Entropy with an increase in temperature is due to the increase in the energy diffusion related to the rotational and vibration energies. And as for the heat of formation, the positive values indicate that the compound is endothermic. The energy gap control of organic semiconductors is important for many applications, for example, light-emitting diode and organic photovoltaic devices.

ORCID IDs

✉ Rosure Borhanalden Abdulrahman, <https://orcid.org/0000-0003-3439-5672>

REFERENCES

- [1] M. Zhu, and C. Yang, Chem. Soc. Rev. **42**, 4963–4976 (2013). <https://doi.org/10.1039/C3CS35440G>
- [2] L. Dou, Y. Liu, Z. Hong, G. Li, and Y. Yang, Chemical Reviews, **115**, 12633–12665 (2015). <https://doi.org/10.1021/acs.chemrev.5b00165>
- [3] Y. Yao, H. Dong, and W. Hu, Advanced Materials, **28**, 4513–4523 (2016). <https://doi.org/https://doi.org/10.1002/adma.201503007>
- [4] H. Bronstein, C.B. Nielsen, B.C. Schroeder, and I. McCulloch, Nature Reviews Chemistry, **4**, 66–77 (2020). <https://doi.org/10.1038/s41570-019-0152-9>
- [5] M. Fröbel, F. Fries, T. Schwab, S. Lenk, K. Leo, M.C. Gather, and S. Reineke, Scientific Reports, **8**, 9684 (2018). <https://doi.org/10.1038/s41598-018-27976-z>
- [6] D.-H. Kim, A. D'Aléo, X.-K. Chen, A. D. S. Sandanayaka, D. Yao, L. Zhao, T. Komino, E. Zaborova, G. Canard, Y. Tsuchiya, E. Choi, J. W. Wu, F. Fages, J.-L. Brédas, J.-C. Ribierre, and C. Adachi, Nature Photonics, **12**, 98–104 (2018). <https://doi.org/10.1038/s41566-017-0087-y>
- [7] K. Tuong Ly, R.-W. Chen-Cheng, H.-W. Lin, Y.-J. Shiau, S.-H. Liu, P.-T. Chou, C.-S. Tsao, Y.-C. Huang, and Y. Chi, Nature Photonics, **11**, 63–68 (2017). <https://doi.org/10.1038/nphoton.2016.230>
- [8] D. Baran, N. Gasparini, A. Wadsworth, C. H. Tan, N. Wehbe, X. Song, Z. Hamid, W. Zhang, M. Neophytou, T. Kirchartz, C.J. Brabec, J.R. Durrant, and I. McCulloch, Nature Communications, **9**, 2059 (2018). <https://doi.org/10.1038/s41467-018-04502-3>
- [9] M. Ameri, M. Ghaffarkani, R. T. Ghahrizjani, N. Safari, and E. Mohajerani, Solar Energy Materials and Solar Cells, **205**, 110251 (2020). <https://doi.org/https://doi.org/10.1016/j.solmat.2019.110251>
- [10] W. Tang, Y. Huang, L. Han, R. Liu, Y. Su, X. Guo, and F. Yan, Journal of Materials Chemistry C, **7**, 790–808 (2019). <https://doi.org/10.1039/C8TC05485A>
- [11] Y. Huang, E.-L. Hsiang, M.-Y. Deng, and S.-T. Wu, Light: Science and Applications, **9**, 105 (2020). <https://doi.org/10.1038/s41377-020-0341-9>
- [12] T. Okamoto, C. P. Yu, C. Mitsui, M. Yamagishi, H. Ishii, and J. Takeya, Journal of the American Chemical Society, **142**, 9083–9096 (2020). <https://doi.org/https://doi.org/10.1021/jacs.9b10450>
- [13] J. Sun, Y. Choi, Y. J. Choi, S. Kim, J.-H. Park, S. Lee, and J. H. Cho, Advanced Materials, **31**, 1803831 (2019). <https://doi.org/https://doi.org/10.1002/adma.201803831>
- [14] M. Duan, L. Jiang, B. Shao, C. Feng, H. Yu, H. Guo, H. Chen, and W. Tang, Applied Catalysis B: Environmental, **297**, 120439 (2021). <https://doi.org/10.1016/j.apcatb.2021.120439>
- [15] R. Roccanova, A. Yangui, H. Nhalil, H. Shi, M.-H. Du, and B. Saparov, ACS Applied Electronic Materials, **1**, 269–274 (2019). <https://doi.org/10.1021/acsaem.9b00015>
- [16] J. Tao, D. Liu, J. Jing, H. Dong, L. Liu, B. Xu, and W. Tian, Advanced Materials, **33**, 2105466 (2021). <https://doi.org/10.1002/adma.202105466>
- [17] J. D. Yuen, V. A. Pozdin, A. T. Young, B. L. Turner, I. D. Giles, J. Naciri, S. A. Trammell, P. T. Charles, D. A. Stenger, and M. A. Daniele, Dyes and Pigments, **174**, 108014 (2020). <https://doi.org/10.1016/j.dyepig.2019.108014>
- [18] A. G. Macedo, L. P. Christopholi, A. E. X. Gavim, J. F. de Deus, M. A. M. Teridi, A. R. bin M. Yusoff, and W. J. da Silva, Journal of Materials Science: Materials in Electronics, **30**, 15803–15824 (2019). <https://doi.org/10.1007/s10854-019-02019-z>
- [19] M. Zhang, J. Shi, C. Liao, Q. Tian, C. Wang, S. Chen, and L. Zang, Chemosensors, **9**, 1 (2020). <https://doi.org/10.3390/chemosensors9010001>
- [20] É. Torres, M. N. Berberan-Santos, and M. J. Brites, Dyes and Pigments, **112**, 298–304 (2015). <https://doi.org/10.1016/j.dyepig.2014.07.019>
- [21] M. Zhang, Y. Bai, C. Sun, L. Xue, H. Wang, and Z.-G. Zhang, Science China Chemistry, **65**, 462–485 (2022). <https://doi.org/10.1007/s11426-021-1171-4>
- [22] K. Nie, X. Peng, W. Yan, J. Song, and J. Qu, Journal of Bio-X Research, **3**, 174–182 (2020). <https://doi.org/10.1097/JBR.0000000000000081>
- [23] A. Sugie, W. Han, N. Shioya, T. Hasegawa, and H. Yoshida, The Journal of Physical Chemistry C, **124**, 9765–9773 (2020). <https://doi.org/10.1021/acs.jpcc.0c01743>
- [24] P. Bultinck, T. Kuppens, X. Gironés, and R. Carbó-Dorca, Journal of Chemical Information and Computer Sciences, **43**, 1143–1150 (2003). <https://doi.org/10.1021/ci0340153>
- [25] G. Halder, *Introduction to chemical engineering thermodynamics*, 2nd ed (PHI Learning Pvt. Ltd., 2014).

- [26] B. Schrader, ed., *Infrared and Raman spectroscopy: methods and applications* (John Wiley & Sons, 2008).
- [27] S. Aronson, B. Strumeyer, and R. Goodman, *The Journal of Physical Chemistry*, **76**, 921–925 (1972). <https://doi.org/10.1021/j100650a024>
- [28] J. I. Gersten and F. W. Smith, *The physics and chemistry of materials* (Toronto: Wiley New York, 2001).
- [29] C.-G. Zhan, J. A. Nichols, and D. A. Dixon, *The Journal of Physical Chemistry A*, **107**, 4184–4195 (2003). <https://doi.org/10.1021/jp0225774>
- [30] Siyamak Shahab and Masoome Sheikhi, *Russian Journal of Physical Chemistry B*, **14**, 15–18 (2020). <https://doi.org/https://doi.org/10.1134/S1990793120010145>
- [31] W. D. Callister and D. G. Rethwisch, *Materials science and engineering: an introduction*, 10th ed (New York: Wiley, 2018).
- [32] J. Bouwman, P. Castellanos, M. Bulak, J. Terwisscha van Scheltinga, J. Cami, H. Linnartz, and A. G. G. M. Tielens, *Astronomy and Astrophysics*, **621**, A80 (2019). <https://doi.org/https://doi.org/10.1051/0004-6361/201834130>
- [33] R. M. Kubba, M. U. Al-Dilemy, and M. Shanshal, *National Journal of Chemistry*, **38**, 293–310 (2010).
- [34] J. M. Dixon, M. Taniguchi, and J. S. Lindsey, *Photochemistry and Photobiology*, **81**, 212–213 (2007). <https://doi.org/10.1111/j.1751-1097.2005.tb01544.x>
- [35] G. Blanquart, and H. Pitsch, *The Journal of Physical Chemistry A*, **111**, 6510–6520 (2007). <https://doi.org/10.1021/jp068579w>

**НАПІВЕМПІРИЧНЕ ДОСЛІДЖЕННЯ ЕЛЕКТРОННИХ, КОЛИВАЛЬНИХ ТА ТЕРМОДИНАМІЧНИХ
ВЛАСТИВОСТЕЙ МОЛЕКУЛИ ПЕРИЛЕНУ (C₂₀H₁₂)**

Абдул Хакім Ш. Мохаммед^а, Ісса З. Хассан^а, Хасан А. Кадхем^б, Росуре Борханалден Абдулрахман^с

^аФакультет фізики, освітній коледж чистих наук, університет Кіркука, Кіркук, Ірак

^бМіністерство освіти, відкритий освітній коледж, Кіркук центр, Ірак

^сФакультет фізики, науковий коледж, університет Кіркука, Кіркук, Ірак

В роботі методом обчислювання досліджено спектроскопічні та термодинамічні властивості молекули перилену (C₂₀H₁₂) у газовій фазі за допомогою програм напівемпіричного методу [Nucor Chem8.0 і WinMoras7.0] через (MNDO-PM3). Цей спосіб забезпечує більшу простоту і швидкість роботи. Були розраховані електронні властивості, такі як повна енергія, енергія дисоціації, молекулярна орбіталь, потенціали іонізації, електронна спорідненість та енергетична щільність. Також були розрахований УФ-видимий спектр та проведено вібраційний аналіз. Крім того, були розраховані термодинамічні властивості при стандартній температурі, такі як теплота утворення, ентропія, ентальпія, теплоємність і вільна енергія Гіббса.

Ключові слова: перилен; C₂₀H₁₂; енергія молекули; видимий УФ; ІЧ; MNDO-PM3; термодинаміка